Journal of Nanostructure in Chemistry (2018) 8:413–420
https://doi.org/10.1007/s40097-018-0274-5

ORIGINAL RESEARCH

Synthesis and characterization of brominated poly(2,6-diphenyl-*p*-phenylene oxide)/SiO_2 nanocomposite membrane for CO_2/N_2 separation

Hojjat Ghanbarian[1] · **Behrooz Mirza**[2]

Received: 17 May 2018 / Accepted: 28 July 2018 / Published online: 19 August 2018

Abstract

Synthesized poly(2,6-diphenyl-*p*-phenylene oxide) ($PPPO_{dp}$) and brominated poly(2,6-diphenyl-*p*-phenylene oxide) ($BPPPO_{dp}$) are identified as new membranes for CO_2/N_2 separation and characterized by SEM, FTIR, and ^{1}HNMR. $BPPPO_{dp}$ is known as a flexible membrane with higher permselectivity ($\alpha_{CO_2/N_2} = 30.53$) than $PPPO_{dp}$ membranes. BPPPO and SiO_2 nanocomposite membranes display improved CO_2 permeability and CO_2/N_2 selectivity compared to the pure $PPPO_{dp}$, and $BPPPO_{dp}$ membranes. The CO_2/N_2 separation mechanism in the membranes is related to the amount of gas dissolution than the amount of gas diffusion.

Graphical abstract

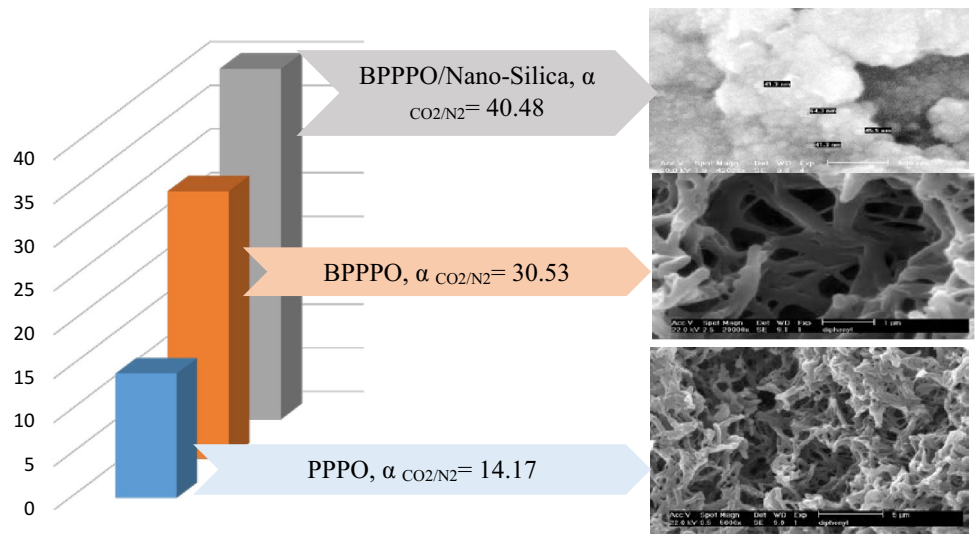

Keywords Poly(2,6-diphenyl-*p*-phenylene oxide) membrane · Brominated poly(2,6-diphenyl-*p*-phenylene oxide) membrane · Brominated poly(2,6-diphenyl-*p*-phenylene oxide)/SiO_2 nanocomposite membrane · Gas separation

✉ Behrooz Mirza
b.mirza@kiau.ac.ir; b_mirza@azad.ac.ir

[1] Department of Science, South Tehran Branch, Islamic Azad University, Tehran, Iran

[2] Department of Chemistry, Karaj Branch, Islamic Azad University, Karaj, Iran

Introduction

One of the straightest techniques to decrease the global warming effect due to atmospheric CO_2 increase is found in CO_2 removal from gaseous streams which is produced in the production of energy from industrial processes [1, 2]. Using

membrane technology in gas separation has created great revolution compared to traditional separation processes [3, 4].That is owing to their low cost, excellent efficiency and being trustworthy.

Recently, three popular gas separation membranes including polymeric membrane, inorganic membrane and new block polymeric membrane are used extensively for CO_2 separation. However, all of them have some defects to industrialization [5]. Highly permeable inorganic membranes suffer from brittle structure, structure defects and also high costs. Therefore, preparation, characterization, and application of inorganic separation membranes were just limited to the laboratory. While, polymeric separation membranes attract more and more attention because of the no expensive and easily fabricated materials. The modified polymeric membranes display improved permeability and CO_2 selectivity. Polymeric membranes are commonly used for CO_2 separation because of their extensive applications: separation of CO_2/H_2 in gas refinement, separation of CO_2/N_2 in carbon capture, separation of CO_2/CH_4 in natural gas refinement, separation of CO_2/O_2 in food packaging [6].

The mechanism of gas separation is distinguished by size sieving because of the rigid chain structures of the polymer matrix [7]. Polymeric membranes with great permeability and selectivity are difficult to prepare.

Poly(2,6-dimethyl-*p*-phenyleneoxide) ($PPPO_{dm}$) as a glassy polymeric material is introduced suitably as a gas separation membrane, because of the great permeability and suitable selectivity [1]. In particular, $PPPO_{dm}$ membrane with great CO_2 permeability (~ 40 bar) and great CO_2/N_2 selectivity (~ 15) is preferred to other glassy polymers [8]. Chemically modified membranes such as brominated poly(2,6-dimethyl-*p*-phenyleneoxide) ($BPPPO_{dm}$) could often improve the gas permeability and selectivity [9, 10].

Addition of nanosized fillers to the polymer matrix could improve the separation performance of polymeric materials through modifying the chain packing of the polymer [1, 11]. Nano-scaled fillers like to be adjusted to the chain packing of glassy polymers in a way that increases the permselectivity trough creating additional selective free holes.

The SiO_2, TiO_2 and MoS_2 nanoparticles through polymer chain interruption bring improvement in gas separation. Polymeric membrane with dispersing nanoparticles is usually challenging due to undesirable interactions between the polymeric matrix and inorganic nano fillers. The appropriate polymer selection and applying the useful inorganic nanoparticle are two essential issues to get useful polymeric membranes [12].

Among different inorganic nanoparticles, SiO_2 nanoparticles are identified as an appropriate modifier for gas separation membranes owing to their high specific surface area and the ability of chemical functionalization, high mechanical and thermal stabilities [12–16].

Merkel et al. introduced poly(4-methyl-2-pentyne)(PMP)/silica nanocomposite including silica NPs (30 wt%), as more effective membrane than pure PMP at gas separation [17]. Also poly(amide-6-b-ethylene oxide) (PEBAX) including 27 wt% silica NPs displayed 277 bar for CO_2 permeability of and 79 for α_{CO_2/N_2} selectivity [18].

With regard to the previous literature, here, we synthesized poly(2,6-diphenyl-*p*-phenylene oxide) (PPPO), brominated poly(2,6-diphenyl-*p*-phenylene oxide) (BPPPO), and BPPPO/SiO_2 nanocomposite as suitable porous membrane for CO_2 adsorption (Fig. 1).

Experimental

Materials

PPO_{dm} (M_n 25,000, polydispersity 2.0), N,N,N′,N′ tetramethylethylenediamine (TMEDA, 99%), 2,6-diphenylphenol (98%), bromine (Br_2, 99.5%), chloroform ($CHCl_3$, 99.8%), ethanol (99.8%), methanol (99.8%), anhydrous hydrazine (98%), 1,2-dichlorobenzene (98.5%), chlorosulfonic acid (99%), anhydrous magnesium sulfate (99.5%), glacial acetic acid (99.8%) and silica nanopowders (SiO_2, 99.5%, 10 nm) and copper (I) chloride (CuCl, 98.5%) from Aldrich.

Synthesis of $PPPO_{dp}$

The synthesis of $PPPO_{dp}$ was performed according to reported procedure [19]. In a 100 cc flask, CuCl (0.041 g), TMEDA (0.031 g), and anhydrous magnesium sulfate (2 g) are added to 1,2-dichlorobenzene (35 cc). The mixture is heated in an oil bath at 65 °C under magnetic stirring. Oxygen is bubbled into the mixture for 15 min. After green color observation in solution, 40 cc of 2,6-diphenylphenol solution is added dropwise during 20 min and made a dark red color immediately. After 24 h, several drops of anhydrous hydrazine are added to the solution to remove byproducts. The inorganic solids are filtered, and the solution is added dropwise to methanol (400 cc) including hydrazine and the solution is shaken for several hours. Then produced polymer is filtered and resolved in chloroform (40 cc) and precipitated in methanol (400 cc). The 3 g of polymer with M_n ~ 120,000 is collected by filtration and dried at 80 °C under vacuum for 24 h. The density of PPPO is ~ 1.11 g cm^{-3} measured by an excluded volume method at room temperature.

Synthesis of $BPPPO_{dp}$

For synthesis of BPPPO, PPPO (5 g) and $CHCl_3$ (50 cc) are added to a 100 cc flask. The mixture is stirred with a magnetic stirrer. The 20 cc of bromine solution included Br_2 (10 cc) and $CHCl_3$ (10 cc), is added dropwise to the mixture

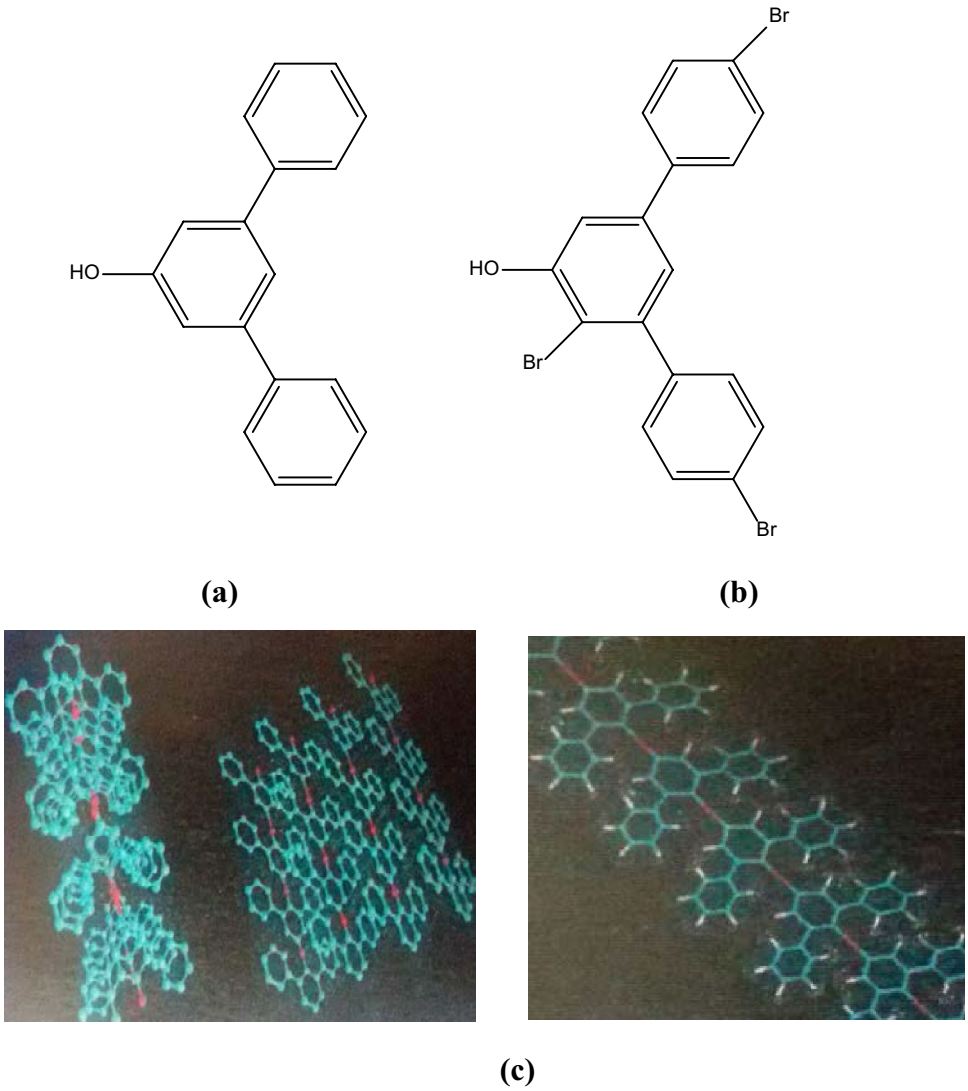

Fig. 1 The monomer structure of poly(2,6-diphenyl-*p*-phenylene oxide) ($PPPO_{dp}$) (**a**); and brominated poly(2,6-diphenyl-*p*-phenylene oxide) ($BPPPO_{dp}$) (**b**); and three-dimensional model of poly(2,6-diphenyl-*p*-phenylene oxide) ($BPPPO_{dp}$) (c)

during 30 min under Argon atmosphere. After 1 h stirring at room temperature, 800 cc ethanol is added under mechanical stirring and the BPPPO is precipitated out. The produced polymer is filtered and dried at room temperature under vacuum. The extent of bromination is 80–95% from NMR spectrum. The density of BPPPO is ~ 1.43 g cm^{-3} measured by the excluded volume method at room temperature with M_n ~ 180,000.

Membrane preparation

The $PPPO_{dp}$, $BPPO_{dp}$, and $BPPPO_{dp}/SiO_2$ nanocomposite membranes are fabricated. The solution of PPPO (3 wt%, in $CHCl_3$) is cast on glass plate at room temperature. Similarly, the BPPPO membrane is prepared.

The BPPPO/silica membrane is prepared as follows: 0.3 g BPPPO is dissolved in 5 cc $CHCl_3$ under stirring. Silica NPs (10 nm) is added slowly to the BPPPO solution. The mixture is vigorously stirred with 1150 rpm for 15 min to dispersion. Then mixture is cast onto a plate at room temperature to dry. After drying, the resulting membranes, with 55–85 μm thickness, are peeled off and stored in a desiccator for testing.

Adding nanoparticles to glassy polymer membranes increases the gas permeability through disturbed polymer chain packing and then increase free volume of membranes.

Gas separation experiments

The membranes gas permeability is examined using a constant-volume setup (Fig. 2). The test setup is made of two compartment stainless steel cells in a way that a flat circular membrane with an effective area of 10.45 cm^2, and a reticular steel support are placed between two flanges and held by O-rings to avoid gas leakage. The experiments are started by vacating the cell up to − 0.1 bar for sending out any remaining gases before using feeding gases, which is to avoid further measurement errors. The rate of permeation

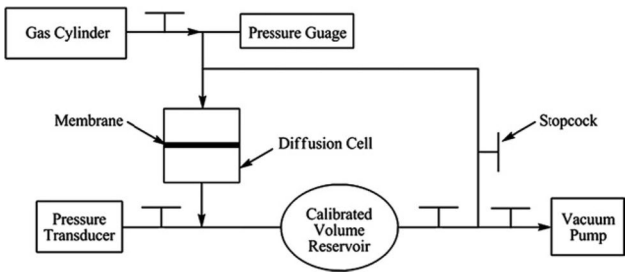

Fig. 2 Schematic illustration of the constant-volume variable-pressure permeation test setup

(Barrer) is calculated from the pressure changes on the permeate side versus time, according to the following equation (1 Barrer = 10^{-10} cm^3 (STP)-cm/cm^2 s cmHg):

$$P = \frac{273 \times 10^{10}}{760} \frac{VL}{AT\left(\frac{p_2 \times 76}{14.7}\right)} \left(\frac{dp}{dt}\right)$$

where V refers to the volume of the permeate side in cm, L and A represent membrane thickness (cm) and the effective area (cm^2), and T is the absolute temperature. p_2 is the feed pressure of the upstream in bar and dp/dt is the slope of permeate pressure change versus time, in its steady state (linear) region.

Permeability data of CO_2 and N_2 is measured for three times, and the average values are reported. The membranes CO_2/N_2 ideal selectivity (α_{CO_2/N_2}) is determined as the ration of CO_2 permeation to N_2 permeation using the following equation: $\alpha = P_{CO_2}/P_{N_2}$; where P_{CO_2} and P_B are related to the permeabilities of pure CO_2 and N_2, respectively [20–22].

Characterization

Scanning electron microscope (SEM) (Philips 505) is used to detect the morphology and particle dispersion in all three membranes. The SEM is used at 10 kV operation voltage. FTIR spectra of pure $PPPO_{dp}$, and $BPPO_{dp}$ are obtained with a FTIR spectrometer (Thermoscientific Nicolet 6700) in the range of 4000–400 cm^{-1}. The solution of $PPPO_{dp}$, and $BPPO_{dp}$ in $CDCl_3$ (~2% w) are used for ^{1}HNMR analyses on a Bruker Advance DRX-400 spectrometer.

Result and discussion

Characterization of PPPO, BPPPO, and BPPPO/SiO_2 nanocomposite and their membranes

Differential scanning calorimetry (DSC)

Thermal properties of the white crystalline $PPPO_{dp}$, and yellowish crystalline $BPPPO_{dp}$ are investigated by DSC analysis (Table 1). To eliminate the influences of less favorable crystal phases are formed at 248 °C, 288 °C for PPPO, BPPPO, respectively. Higher Tg of $BPPPO_{dp}$ is related to three bulky bromine groups in each monomer unit. The second heating run as their melting point are considered at 470 and > 500 °C for PPPO and BPPPO that confirm their crystalline structures.

Table 1 DSC testing results of poly(2,6-diphenyl-*p*-phenylene oxide) ($PPPO_{dp}$); and brominated poly(2,6-diphenyl-*p*-phenylene oxide) ($BPPPO_{dp}$)

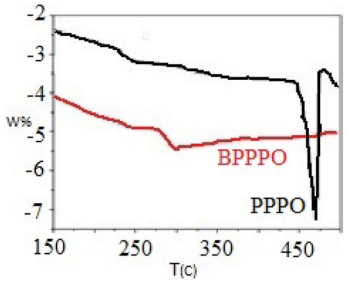

Sample	M_n	Solvent	Approximate density (g/cc)	T_g (°C)	T_m (°C)
PPPO	~ 120,000	$CHCl_3$	~ 1.11	248	470
BPPPO	~ 180,000	$CHCl_3$	~ 1.33	288	– 500

The scanning electron microscope image (SEM)

The gas transport properties strongly depend on the membranes morphology. The cross section morphology of the neat $PPPO_{dp}$, $BPPPO_{dp}$, and $BPPPO_{dp}$/silica nanocomposite membranes are investigated via SEM images (Fig. 3). Figure 3a show porous structure for $PPPO_{dp}$ membrane while Fig. 3b displays optimized porous structure with fewer surface defects for its relatively brominated membrane ($BPPPO_{dp}$). Adding silica nanoparticles to the brominated membrane ($BPPPO_{dp}$) propel it to an agglomerated $BPPPO_{dp}$/silica nanocomposite membrane (Fig. 3c). The nanocomposite membranes with their hydrophilic characterization of silica nanoparticles prefer to agglomerate. Hence $BPPPO_{dp}$/silica nanocomposite membrane seems to appear more selective due to its high density.

FT-IR

Functional groups on the surface of poly(2,6-diphenyl-*p*-phenylene oxide) $PPPO_{dp}$ and brominated poly(2,6-diphenyl-*p*-phenylene oxide) ($BPPPO_{dp}$) are investigated by means of FTIR spectra (Fig. 4). The observed peaks at 1400–1600 cm^{-1} are assigned to the C–C stretching bands of the aromatic rings. $PPPO_{dp}$ reveals that some of the CH

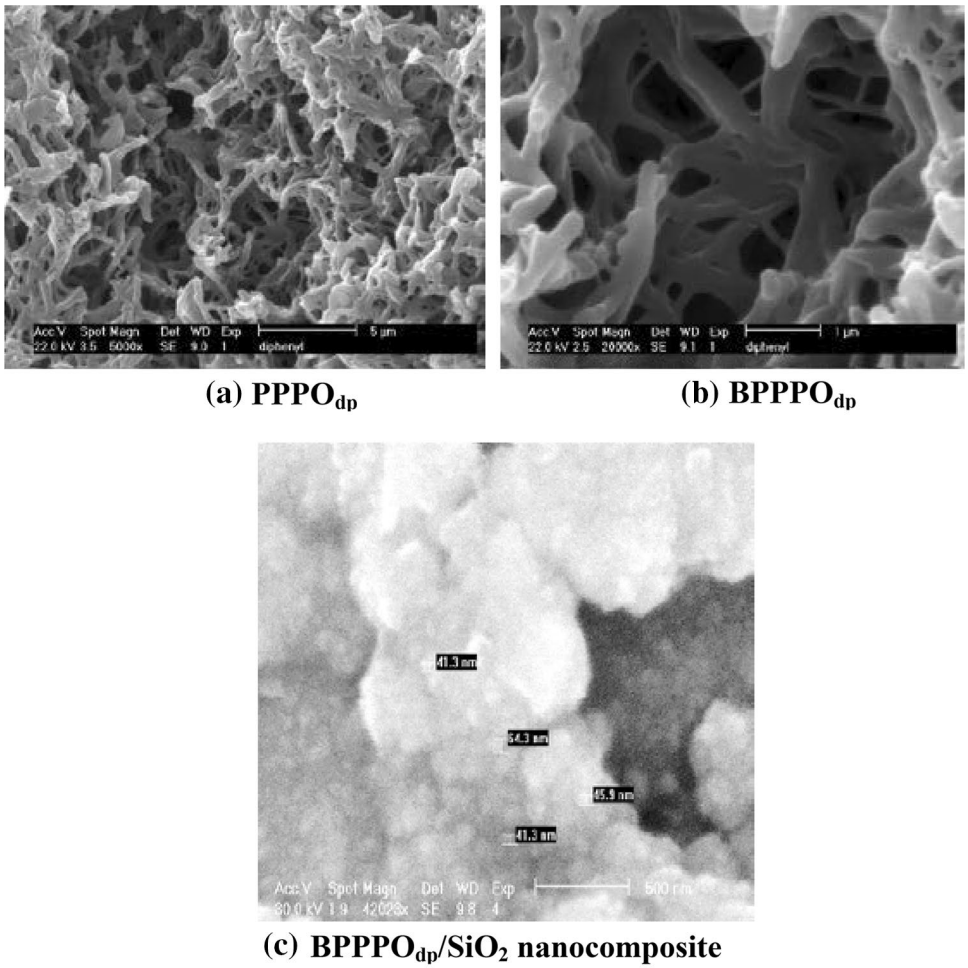

Fig. 3 The SEM image of poly(2,6-diphenyl-*p*-phenylene oxide) (PPPO$_{dp}$) (**a**), brominated poly(2,6-diphenyl-*p*-phenylene oxide) (BPPPO$_{dp}$) (**b**), and BPPPOdp/SiO$_2$ nanocomposite membranes (**c**)

stretching of aromatic rings at 3025 cm^{-1} (Fig. 4a). In addition, the observed peaks at 695 cm^{-1}, and 1147 cm^{-1} corresponds to out of plane bending aromatic CH and C–O stretching bond.

As mentioned before, the observed peaks at 1400, 1600 cm^{-1} illustrate aromatic CC stretching, 3058 cm^{-1} clarify aromatic CH stretching, and 1183 cm^{-1} show out of plane bending aromatic CH bond for brominated poly(2,6-diphenyl-*p*-phenylene oxide) (BPPPO$_{dp}$). Also, monitored peaks around 1030–1050 and 1183 cm^{-1} imply C–Br and C–O stretching bond, respectively.

Nuclear magnetic resonance (NMR)

In ^{1}HNMR spectrum of poly(2,6-diphenyl-*p*-phenylene oxide) (PPPO$_{dp}$) seen some peaks at 6.28 (2H, C_6H_2O), 6.96, 7.1–7.3 ppm (10H, 2 C_6H_5) (Fig. 5a). While, brominated poly(2,6-diphenyl-*p*-phenylene oxide) (BPPPO$_{dp}$) demonstrate some peaks at 6.32 (1H, C_6HOBr), 6.75 and 7.4–7.8 ppm (8H, 2 C_6H_4Br) (Fig. 5b). As seen, decrease of the number of hydrogen atoms in brominated poly(2,6-diphenyl-*p*-phenylene oxide) (BPPPO$_{dp}$) could confirm the new structure from brominating (Fig. 5b).

Gas separation performance test

Three prepared membranes of PPPO$_{dp}$, BPPPO$_{dp}$, BPPPO$_{dp}$/SiO$_2$ nanocomposite are used in the gas separation test (Table 2). According to previous works, the permeability of pure gas is measured in a constant-volume variable-pressure unit and the permselectivity (α) is determined from the following formula: $\alpha = P_A/P_B$; where P_A and P_B are related to the permeabilities of pure gases A and B, respectively (Fig. 2, Table 2) [20–22].

The brominated poly(2,6-dimethyl-1,4-phenylene oxide) (BPPPO$_{dp}$) flexible membrane is identified with lower permeability of CO_2 ($P_{CO_2} = 58$ Barrer) but higher selectivity ($\alpha_{CO_2/N_2} = 30.53$) than poly(2,6-dimethyl-1,4-phenylene oxide)

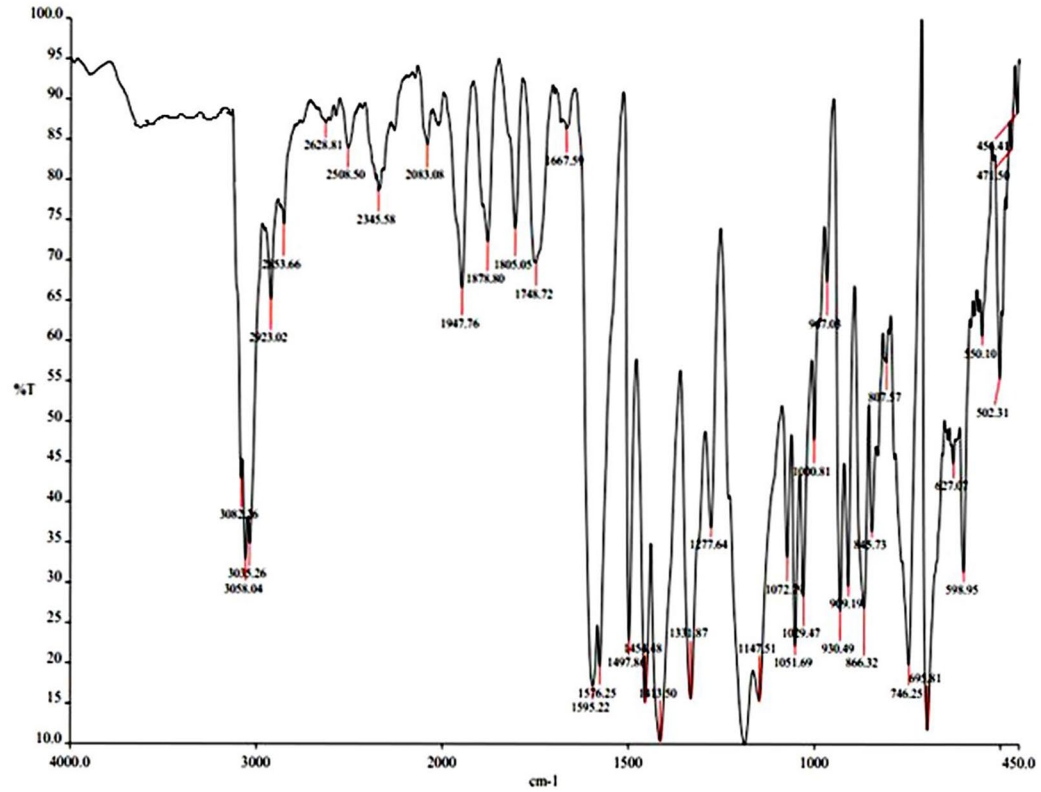

(a) $PPPO_{dp}$

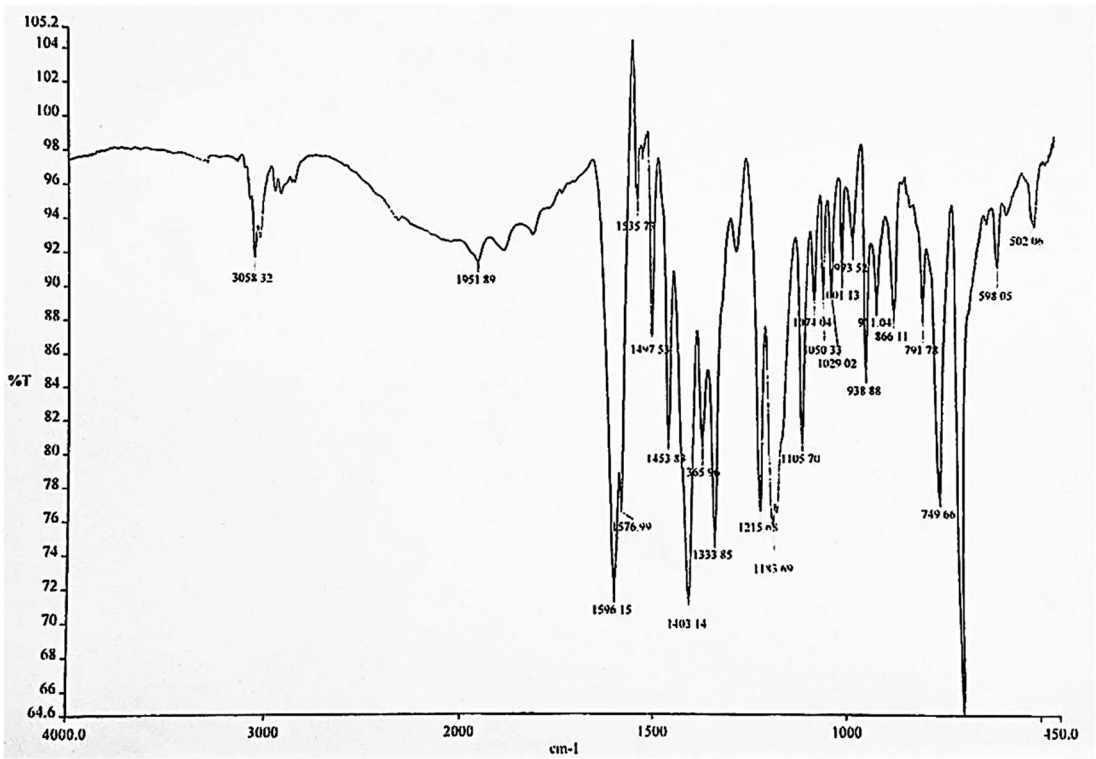

(b) $BPPPO_{dp}$

Fig. 4 The FT-IR of poly(2,6-diphenyl-*p*-phenylene oxide) ($PPPO_{dp}$) (**a**), and brominated poly(2,6-diphenyl-*p*-phenylene oxide) ($BPPPO_{dp}$) (**b**)

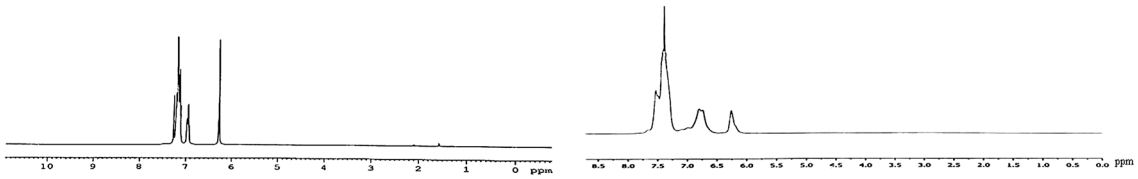

Fig. 5 The NMR spectrum of poly(2,6-diphenyl-*p*-phenylene oxide) (PPPO$_{dp}$) (**a**), and brominated poly(2,6-diphenyl-*p*-phenylene oxide) (BPPPO$_{dp}$) (**b**)

Table 2 Gas separation performance of poly(2,6-diphenyl-*p*-phenylene oxide) (PPPO$_{dp}$), brominated poly(2,6-diphenyl-*p*-phenylene oxide) (BPPPO$_{dp}$), and BPPPOdp/SiO$_2$ nanocomposite

Membranes	P_{CO_2} (bar)	P_{N_2} (bar)	α_{CO_2/N_2}
PPPO$_{dp}$	68	4.8	14.17
BPPPO$_{dp}$	58	1.9	30.53
BPPPO/nano-silica	85	2.1	40.48

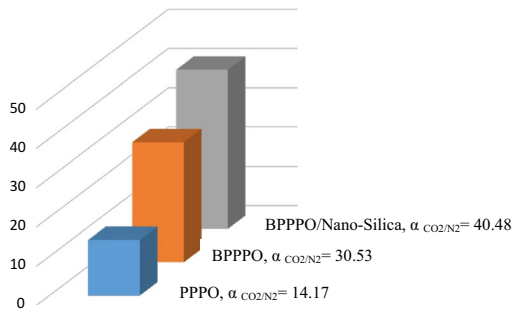

Fig. 6 The permselectivity diagram (α_{CO_2/N_2}) of poly(2,6-diphenyl-*p*-phenylene oxide) (PPPO$_{dp}$) (blue), brominated poly(2,6-diphenyl-*p*-phenylene oxide) (BPPPO$_{dp}$) (orange), and BPPPOdp/SiO$_2$ nanocomposite membranes (gray) (according to the calculation in Table 2)

(PPPO$_{dm}$) membranes with permeability of CO_2 (P_{CO_2} = 68 Barrer) and selectivity (α_{CO_2/N_2} = 14.7) (Table 2, Fig. 6). Thus, BPPPO$_{dp}$ is selected as a beginning material for manufacture process of polymer/SiO$_2$ nanocomposite membrane. The BPPPO$_{dp}$/SiO$_2$ nanocomposite membrane including 10 wt% silica NPs present a greatly enhanced CO_2 permeability in (P_{CO_2} = 85 Barrer) and (α_{CO_2/N_2} = 40.48). Hence they are found more effective than poly(4-methyl-2-pentyne)(PMP)/silica nanocomposite with permeability and selectivity for large organic molecules [17]. Meanwhile poly(amide-6-b-ethylene oxide)/silica nanocomposite displayed 277 bar permeability of CO_2 and α_{CO_2/N_2} = 79 [18].

The study of mechanism demonstrates the silica nanoparticles owing to their incompatibility with polymer chains produce some gaps in the structure of nanocomposite, which results in enhanced permeability [19]. The surface of silica

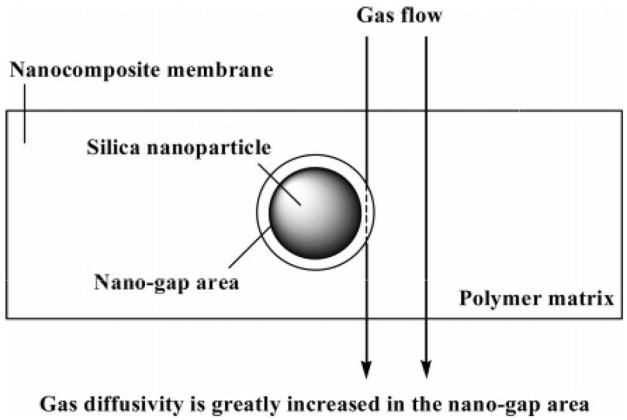

Fig. 7 Illustration of nanogap formation in the BPPOdp/silica nanocomposite membranes

NPs with polar silano groups displayed low compatibility with the BPPO$_{dp}$ matrix that causes silica particles to aggregate in the membrane. A narrow gap around the silica NPs formed due to lack of tight interaction between polymer chains and silica NPs, which made high gas diffusivity and permeability (Fig. 7).

Conclusion

Poly(2,6-diphenyl-*p*-phenylene oxide) (PPPO$_{dp}$), brominated poly(2,6-diphenyl-*p*-phenylene oxide) (BPPPO$_{dp}$), and BPPPOdp/SiO$_2$ nanocomposite are synthesized and compared together in CO_2 permeability and CO_2/N_2 permselectivity. BPPPO$_{dp}$ membranes are known to be more efficient than PPPO$_{dp}$ through higher CO_2/N_2 permselectivity. The BPPPO$_{dp}$/SiO$_2$ nanocomposite membrane with the highest CO_2 permeability and CO_2/N_2 permselectivity is introduced as the most effective membrane. The CO_2 permeability increase through silica addition to the membrane.

References

1. Rea, R., Ligi, S., Christian, M., Morandi, V., Giacinti Baschetti, M., De Angelis, M.: Permeability and selectivity of PPO/graphene composites as mixed matrix membranes for CO_2 capture and gas separation. Polymers. **10**, 129–148 (2018)
2. Bains, P., Psarras, P., Wilcox, J.: CO_2 capture from the industry sector. Prog. Energy Combust. Sci. **63**, 146–172 (2017)
3. George, G., Bhoria, N., AlHallaq, S., Abdala, A., Mittal, V.: Polymer membranes for acid gas removal from natural gas. Sep. Purif. Technol. **158**, 333–356 (2016)
4. Hou, J., Zhang, H., Hu, Y., Li, X., Chen, X., Kim, S., Wang, Y., Simon, G.P., Wang, H.: Carbon nanotube networks as nanoscaffolds for fabricating ultrathin carbon molecular sieve membranes. ACS Appl. Mater. Interfaces. **10**, 20182–20188 (2018)
5. Li, H., Ding, X., Zhang, Y., Liu, J.: Porous graphene nanosheets functionalized thin film nanocomposite membrane prepared by interfacial polymerization for CO_2/N_2 separation. J. Memb. Sci. **543**, 58–68 (2017)
6. Sodeifian, G., Raji, M., Asghari, M., Rezakazemi, M., Dashti, A.: Polyurethane-SAPO-34 mixed matrix membrane for CO_2/CH_4 and CO_2/N_2 separation. Chin. J. Chem. Eng. (2018). https://doi.org/10.1016/j.cjche.2018.03.012
7. Wang, Y., Li, H., Dong, G., Scholes, C., Chen, V.: Effect of fabrication and operation conditions on CO_2 separation performance of PEO–PA block copolymer membranes. Ind. Eng. Chem. Res. **54**, 7273–7283 (2015)
8. Sridhar, S., Smitha, B., Ramakrishna, M., Aminabhavi, T.M.: Modified poly(phenylene oxide) membranes for the separation of carbon dioxide from methane. J. Memb. Sci. **280**, 202–209 (2006)
9. Hamad, F., Matsuura, T.: Performance of gas separation membranes made from sulfonated brominated high molecular weight poly(2,4-dimethyl-l,6-phenylene oxide). J. Memb. Sci. **253**, 183–189 (2005)
10. Cong, H., Yu, B., Tang, J., Zhao, X.S.: Ionic liquid modified poly(2,6-dimethyl-1,4-phenylene oxide) for CO_2 separation. J. Polym. Res. **19**, 9761–9769 (2012)
11. Chu, L., Deng, S., Zhao, R., Deng, J., Kang, X.: Comparison of adsorption/desorption of volatile organic compounds (VOCs) on electrospun nanofibers with tenax TA for potential application in sampling. PLoS One **11**(10), e0163388 (2016)
12. Aghaei, Z., Naji, L., Hadadi Asl, V., Khanbabaei, G., Dezhagah, F.: The influence of fumed silica content and particle size in poly (amide 6-b-ethylene oxide) mixed matrix membranes for gas separation. Sep. Purif. Technol. **199**, 47–56 (2018)
13. Zargar, V., Asghari, M., Afsari, M.: Gas separation properties of swelled nanocomposite chitosan membranes cross-linked by 3-aminopropyltriethoxysilane. Int. J. Environ. Sci. Technol. (2017). https://doi.org/10.1007/s13762-017-1554-1
14. Ghaee, A., Ghadimi, A., Sadatnia, B., Ismail, A.F., Mansourpour, Z., Khosravi, M.: Synthesis and characterization of poly(vinylidene fluoride) membrane containing hydrophobic silica nanoparticles for CO_2 absorption from CO_2/N_2 using membrane contactor. Chem. Eng. Res. Des. **120**, 47–57 (2017)
15. Isanejad, M., Mohammadi, T.: Effect of amine modification on morphology and performance of poly (ether-block-amide)/fumed silica nanocomposite membranes for CO_2/CH_4 separation. Mater. Chem. Phys. **205**, 303–314 (2018)
16. Ghadimi, A., Mohammadi, T., Kasiri, N.: Gas permeation, sorption and diffusion through PEBA/SiO_2 nanocomposite membranes (chemical surface modification of nanoparticles). Int. J. Hydrogen Energy **40**, 9723–9732 (2015)
17. Merkel, T.C., Freeman, B.D., Spontak, R.J., He, Z., Pinnau, I., Meakin, P., Hill, A.J.: Ultrapermeable, reverse-selective nanocomposite membranes. Science. **296**, 519–522 (2002)
18. Kim, J.H., Lee, Y.M.: Gas permeation properties of poly(amide-6-*b*-ethylene oxide)–silica hybrid membranes. J. Memb. Sci. **193**, 209–225 (2001)
19. Yu, B., Cong, H., Zhao, X.: Hybrid brominated sulfonated poly(2,6-diphenyl-1,4-phenylene oxide) and SiO_2 nanocomposite membranes for CO_2/N_2 separation. Proc. Natl. Sci. Mater. **22**, 661–667 (2012)
20. Cong, H., Yu, B.: Aminosilane cross-linked PEG/PEPEG/PPEPG membranes for CO_2/N_2 and CO_2/H_2 separation. Ind. Eng. Chem. Res. **49**, 9363–9369 (2010)
21. Koros, W.J., Chan, A.H., Paul, D.R.: Sorption and transport of various gases in polycarbonate. J. Memb. Sci. **2**, 165–190 (1977)
22. Felder, R.M., Huvard, G.S.: 17. Permeation, diffusion, and sorption of gases and vapors. In: Fava, R.A. (ed.) Methods in Experimental Physics, vol. 16, pp. 315–377. Academic, New York (1980)